HHS Public Access

Author manuscript

Otol Neurotol. Author manuscript; available in PMC 2016 July 01.

Published in final edited form as:

Otol Neurotol. 2015 July ; 36(6): 953–960. doi:10.1097/MAO.0000000000000786.

Non-ototoxic local delivery of bisphosphonate to the mammalian cochlea

Woo Seok Kang, M.D., Ph.D.[1,2,3], **Shuting Sun, Ph.D.**[4], **Kim Nguyen, B.S.**[4], **Boris Kashemirov, Ph.D.**[4], **Charles E. McKenna, Ph.D.**[4], **S. Adam Hacking, Ph.D.**[5], **Alicia M. Quesnel, M.D.**[1,2,3], **William F. Sewell, Ph.D.**[2], **Michael J. McKenna, M.D.**[1,2,3,*], and **David H. Jung, M.D., Ph.D.**[1,2,3,*]

[1]Department of Otolaryngology, Massachusetts Eye and Ear Infirmary, Boston, MA, USA

[2]Eaton Peabody Laboratory, Massachusetts Eye and Ear Infirmary, Boston, MA, USA

[3]Department of Otology and Laryngology, Harvard Medical School, Boston, MA, USA

[4]Department of Chemistry, University of Southern California, Los Angeles, CA, USA

[5]Department of Orthopaedics, Massachusetts General Hospital, Harvard Medical School, Boston, MA, USA

Abstract

Hypothesis—Local delivery of bisphosphonates results in superior localization of these compounds for the treatment of cochlear otosclerosis, without ototoxicity.

Background—Otosclerosis is a common disorder of abnormal bone remodeling within the human otic capsule. It is a frequent cause of conductive hearing loss from stapes fixation. Large lesions that penetrate the cochlear endosteum and injure the spiral ligament result in sensorineural hearing loss. Nitrogen-containing bisphosphonates (e.g., zoledronate) are potent inhibitors of bone remodeling with proven efficacy in the treatment of metabolic bone diseases, including otosclerosis. Local delivery to the cochlea may allow for improved drug targeting, higher local concentrations, and the avoidance of systemic complications. In this study, we utilize a fluorescently labeled bisphosphonate compound (6-FAM-ZOL) to determine drug localization and concentration within the otic capsule. Various methods for delivery are compared. Ototoxicity is evaluated by ABR and DPOAEs.

Methods—6-FAM-ZOL was administered to guinea pigs via intraperitoneal injection, placement of alginate beads onto the round window membrane (RWM), or microfluidic pump infusion via a cochleostomy. Hearing was evaluated. Specimens were embedded into resin blocks, ground to a mid-modiolar section, and quantitatively imaged using fluorescence microscopy.

Corresponding author: David H. Jung, Department of Otolaryngology, Massachusetts Eye and Ear Infirmary, 243 Charles Street, Boston, MA 02114, Tel: 1-617-523-7900, david_jung@meei.harvard.edu.

*Co-corresponding authors

Financial disclosure: None

Conflict of Interest: Drs. Sun, Kashemirov, and C. E. McKenna are founding members of BioVinc LLC, which is producing 6-FAM-ZOL for commercial use.

Results—There was a dose-dependent increase in fluorescent signal following systemic 6-FAM-ZOL treatment. Local delivery via the RWM or a cochleostomy increased delivery efficiency. No significant ototoxicity was observed following either systemic or local 6-FAM-ZOL delivery.

Conclusions—These findings establish important pre-clinical parameters for the treatment of cochlear otosclerosis in humans.

Keywords

otosclerosis; inner ear drug delivery; bisphosphonates; fluorescence imaging

INTRODUCTION

Otosclerosis is a disease of abnormal bone metabolism and remodeling affecting the otic capsule, which can result in a fixed stapes footplate and clinically present as a conductive hearing loss (1). Stapedectomy surgery and amplification can improve the conductive hearing loss caused by otosclerosis. Cochlear otosclerosis results from an extensive otosclerotic lesion that extends to the cochlear endosteum and spiral ligament (2), resulting in a sensorineural hearing loss (SNHL). It has been estimated that 0.3% of Caucasians experience conductive hearing loss as a result of otosclerosis (3), and that up to 20–30% of these patients further develop the sensorineural hearing loss associated with the more extensive lesions of cochlear otosclerosis (4). Many theories have been proposed to explain the SNHL observed in cochlear otosclerosis, including the release of toxic metabolites into the inner ear and vascular shunts between the otosclerotic focus and spiral capillaries (5), although these ideas remain unproven. Some patients progress to a profound loss and require cochlear implantation, which can pose unique challenges (6–9).

Notably, the prevalence of osteoporosis is significantly higher among patients with otosclerosis (10), an association that may be mediated by a shared polymorphism in the COL1A1 gene (11). Moreover, post-mortem histopathologic examination of temporal bone specimens from adult patients with type I osteogenesis imperfect a reveals otosclerotic lesions (12). Direct links between otosclerosis and Paget's disease have been more elusive, with the largest published study finding no evidence for ossicular fixation in a histopathologic temporal bone study (13). Taken together, the data suggest that the disease-causing mechanisms of otosclerosis share common features with other diseases of bone metabolism.

Medical treatments for other metabolic bone disorders may, therefore, also be efficacious for otosclerosis treatment. In this regard, nitrogen-containing bisphosphonates, including zoledronate, have been used to treat diseases such as osteoporosis, osteogenesis imperfect a and Paget's disease (14). Bisphosphonates concentrate in bone and act in a complex manner to inhibit osteoclast formation, migration, and activity while promoting apoptosis of osteoclasts (15,16). No ototoxicity has been reported in the multiple human trials of zoledronate, which is administered once a year for the treatment of osteoporosis (17). Based on the known efficacy of bisphosphonates in treating other metabolic bone diseases, our group recently reported sensorineural hearing stabilization following zoledronate treatment

of a small number of patients with cochlear otosclerosis, at an average of 13 months' follow-up time (4).

While we did not observe any complications in our small study, the systemic use of nitrogen-containing bisphosphonates is associated with serious toxicities including osteonecrosis of the jaw (ONJ), atypical femur fracture, atrial fibrillation, erosive esophagitis, and renal failure (18), although the association with ONJ is controversial (19). While the incidence of these complications is low (20), some clinicians have proposed the implementation of bisphosphonate "drug holidays" for patients treated with bisphosphonates for osteoporosis but who are at relatively low risk for fractures (21). Moreover, the persistence of nitrogen-containing bisphosphonates, including zoledonate, within bone following systemic administration potentially extends the at-risk period for patients treated with systemic bisphosphonates (22).

Local delivery of bisphosphonates to the inner ear could avoid systemic toxicities and maximize the concentration of drug at its desired target. To that end, we have developed an animal model for delivery of bisphosphonates to the cochlea. A key feature of this model has been the use of a novel derivative of zoledronate, coupled to carboxyfluorescein (6-FAM-ZOL), to provide for direct visualization of bisphosphonate distribution. We demonstrate that local delivery of bisphosphonate via the round window or a cochleostomy can result in levels of fluorescence in the cochlear lateral wall significantly higher than those seen following systemic delivery. Critically, local bisphosphonate delivery to the cochlea in this manner is not ototoxic.

MATERIALS AND METHODS

Animals

Male albino guinea pigs (Hartley strain; Charles River Laboratories, Inc., Wilmington, MA), each weighing approximately 350g, were used. Nembutal (12.5 mg/kg intraperitoneally), Fentanyl (0.1 mg/kg intramuscularly), and Droperidol (5 mg/kg intramuscularly) were given for anesthesia. Supplemental doses of 0.7 mg/kg Fentanyl and 3.0 mg/kg Droperidol alternating with 6.25 mg/kg Nembutal were administered as needed. Animals were euthanized using pentobarbital (Fatal-Plus) at 390 mg/kg. The Massachusetts Eye and Ear Infirmary Institutional Animal Care and Use Committee approved all procedures.

6-FAM-ZOL synthesis

Zoledronate was purchased from Molekula Limited, UK; 5(6)-carboxyfluorescein, succinimidyl ester was purchased from Invitrogen, CA, USA. 6-FAM-ZOL was synthesized as described previously (23,24). The approach is based on attachment of a functionalized epoxide linker to the imidazolyl nitrogen of zoledronate under mild reaction conditions (aqueous, near neutral pH, 21–40 °C). The resulting drug-linker intermediate has an amino group available for reaction with 5(6)-carboxyfluorescein, succinimidyl ester in the next step. The final conjugate, 6-FAM-ZOL was isolated by HPLC (purity > 95 %) and fully characterized by ^{1}H, ^{31}P NMR, HRMS, UV-VIS and fluorescent spectroscopy (23,24). 6-

FAM-ZOL binds to hydroxyapatite with approximately 70% affinity relative to native zoledronate (25).

Hearing measurements

Distortion product otoacoustic emissions (DPOAEs) and auditory brainstem responses (ABRs) were measured in the systemic and RWM delivery experiments. For the cochleostomy experiments, compound action potentials (CAPs) from the auditory nerve were substituted for ABRs. Hearing was measured at 2.78, 4, 5.6, 8, 12, 16, 24, and 32 kHz. See Supplemental Information for complete details.

Systemic drug delivery: intraperitoneal 6-FAM-ZOL injection

We administered doses of 6-FAM-ZOL that corresponded by molar weight to either one or three times the human systemic dose (5 mg injection) of zoledronate recommended for osteoporosis. 6-FAM-ZOL was diluted into 1 mL of artificial perilymph (AP) or phosphate buffered saline (PBS) for injection at 0.185 mg/kg (1X 6-FAM-ZOL) and 0.555 mg/kg (3X 6-FAM-ZOL). AP and PBS were both used as carriers in different experiments and no differences were seen. Animals were anesthetized and a 0.5 cm incision made in the abdomen through which 6-FAM-ZOL was injected into the peritoneum. We injected 1 mL of vehicle alone, either AP or PBS, in the control animals. All guinea pigs underwent DPOAEs and ABRs both at the time of treatment and immediately before being sacrificed. Four independent experiments, each with one vehicle-only control, one 1X, and one 3X animal, were performed with AP and three independent experiments with PBS. The content of AP was: 130 mM NaCl, 3.5 mM KCl, 1.5 mM $CaCl_2$, 5.5 mM glucose, 20 mM HEPES, pH 7.4. PBS was 137 mM NaCl, 2.7 mM KCl, 10 mM Na_2HPO_4, 1.8 mM KH_2PO_4, pH 7.4)

Local drug delivery: placement of 6-FAM-ZOL onto the RWM

A 2% (w/v) solution of sodium alginate was prepared in PBS. 10% (0.1X) and 30% (0.3X) of the human systemic dose by molar weight were tested. For 0.1X 6-FAM-ZOL, 1.3 μL of 4 μg/μL 6-FAM-ZOL was mixed with 1.3 μL of 2% sodium alginate solution. For 0.3X 6-FAM-ZOL, 1 μL of 15 μg/μL 6-FAM-ZOL was mixed with 1.3 μL of 2% sodium alginate solution. A few drops of 0.2 M $CaCl_2$ were placed over this mixture, which then formed a hydrogel with a diameter of 1–2 mm. Each hydrogel was made immediately before use. Five independent experiments were performed, each with one PBS control, one 0.1X, and one 0.3X treated animal (15 animals total).

We visualized the round window via a bullectomy approach and placed the beads within the round window membrane (RWM) niche under direct microscopic visualization. Animals were sacrificed 3 weeks later, after middle ear inflammation from surgery had subsided. DPOAEs and ABRs were first measured while animals were under anesthesia prior to bullectomy and again prior to analysis.

Local drug delivery: 6-FAM-ZOL infusion into the scala tympani via a cochleostomy

A Harvard Apparatus PHD 2000 Infusion Syringe Pump was used to introduce 6-FAM-ZOL into the cochlea. A 500 μL glass syringe, filled with 6-FAM-ZOL dissolved into AP at a concentration of 0.25 μg/μL, was connected via polyetherether ketone (PEEK; Upchurch

Scientific) tubing to an 11 mm length of PTFE (teflon) tubing (201 μm od, 101 μm id). A small bleb approximately 600 μm in diameter was fabricated at a point 3 mm from the distal end using methyltriacetoxysilane (Elmer's Stix All).

We performed a cochleostomy approximately 0.5mm distal to the round window via a bullectomy approach and inserted the PTFE tubing into the scala tympani. Dental cement was used to seal the cochleostomy around the tubing. We infused 1 μL over one minute five times, spaced nine minutes apart. Control animals were treated with AP alone. 0.02X animals were infused with 6-FAM-ZOL at 0.25 μg/μL. 0.04X animals were infused with 6-FAM-ZOL at 0.125 μg/μL + 0.193 μg/μL zoledronate (total 4% of the 1X human zoledronate dose by molar weight). DPOAEs and CAPs were measured at time 0 (after cannula insertion and prior to infusion) and at 3 hrs. In independent experiments, three control animals were treated with AP alone, four animals were treated with AP containing 0.02X 6-FAM-ZOL, and three animals were treated with AP containing 0.04X 6-FAM-ZOL + zoledronate. Untreated animals were used for control tissue fluorescence analyses.

Timing of analyses

In humans, bone deposition and renal excretion rapidly clear zoledronate from plasma, with two half-lives at 0.2 and 1.4 hours, and less than 1% of the drug remaining in plasma after 24 hours (26). All animals were therefore analyzed after maximal bisphosphonate deposition. Systemic delivery animals were analyzed at 48 hrs to account for potential differences between IP (our system) and IV (human) delivery. RW delivery animals were analyzed at 3 weeks to allow middle ear inflammation to subside prior to hearing analysis and to account for transit across the RWM. Intracochlear delivery animals were analyzed at 3 hours as this timepoint allowed for high levels of delivery while avoiding the potential confounding long-term effects of a cochleostomy.

Tissue processing

See Supplemental Information for complete details. Briefly, samples were harvested, fixed, dehydrated, and embedded into methylmethacrylate under vacuum. Embedded samples were ground to the mid-modiolus.

6-FAM-ZOL quantification and data normalization

High-resolution images (1360 by 1024; 16bit) were taken under FITC illumination (470/40 excitation, 495lp dicroic; 525/50 emission) using a Carl Zeiss Axiovert 200 Inverted Microscope. ImageJ (27) was used to quantify the amount of fluorescence within the cochlear wall and modiolus at each half-turn (Figure 1). Background fluorescence, defined as the average amount of fluorescence in an area of the resin block containing no sample, was subtracted from all measurements. Fluorescence remained stable over at least two weeks after grinding if samples were kept in the dark at room temperature. Some images were also collected using a Leica TCS-SP2 confocal microscope. Confocal images were collected over a depth of 500 μm to generate maximum fluorescence images.

Statistical Analysis

Statistical data analysis was performed using the SAS software package. Null hypotheses were rejected at $p>0.05$.

Mixed model analysis of variance was used to analyze the effect of dose on fluorescent response in the cochlea. A separate model was fit for each experiment. The model included a fixed effect of dose and a random effect of dose within each replicate. For each dose level the reported estimated response is the model based least squares mean and standard error of the mean.

Mixed model analysis of variance was used to analyze the effect of dose on fluorescent response in the tibia. The model included a fixed effect of dose and a random intercept within each replicate. For each dose level the reported estimated response is the model based least squares mean and standard error of the mean.

Mixed model analysis of variance was used to analyze the effect of location on fluorescent response in the cochlea. A separate model was fit for each experiment. The model included a fixed effect of dose and location and a random effect of location within each replicate by dose level.

RESULTS

Systemic zoledrenate (6-FAM-ZOL) enters the bone of the cochlea

Because of the presence of the blood-cochlear barrier, we first assessed whether or not systemically administered zoledrenate efficiently enters the bone of the inner ear. To assess this, we compared the deposition of systemically administered 6-FAM-ZOL (a fluorescent derivative of zoledrenate) in the otic capsule with that in the tibia. 6-FAM-ZOL was administered systemically (i.p.) at an equivalent (1X) or triple (3X) amount relative to the human zoledronate dose by molar weight. We observed fluorescent signal above native cochlear autofluorescence in the lateral wall of cochleae derived from both 1X and 3X 6-FAM-ZOL-treated animals (schematic in Figure 1; Figures 2A–C). This fluorescence increased with dose and the differences were statistically significant (Figure 3A). As a comparison with appendicular cortical bone, we also evaluated tibiae harvested from both control and 6-FAM-ZOL-treated animals. We readily detected bright fluorescent green signal within the tibiae of 6-FAM-ZOL-treated animals (Figure 2D–F). Again, differences between control, 1X, and 3X 6-FAM-ZOL were dose-dependent and statistically significant (Figure 3B). Average fluorescence measurements were 50% stronger in tibiae compared to cochleae (approximately 5,800 fluorescence units above control vs 8,800 fluorescence units above control for the 1X systemic dose; Figures 2 and 3). No significant physiological changes were observed by ABR and DPOAE (Supp. Figure 1). We concluded from these findings that systemic 6-FAM-ZOL treatment resulted in a non-ototoxic, dose-dependent increase in fluorescent signal within otic capsule bone and appendicular cortical bone, with more deposition in cortical bone than in otic capsule bone.

Zoledrenate (6-FAM-ZOL) can enter the bone of the cochlea with round window application

Next, we assessed the distribution of 10% of the 1X systemic dose (0.1X) and 30% of the 1X systemic dose (0.3X) of 6-FAM-ZOL delivered to the RWM. Placement on the round window membrane of an alginate bead containing 0.3X 6-FAM-ZOL resulted in delivery of 6-FAM-ZOL throughout the lateral wall of the cochlea at levels comparable to the 1X systemic dose, while administration of 0.1X 6-FAM-ZOL to the round window membrane resulted in lower, but still detectable, fluorescence (Figure 4A–C). When plotted as a function of distance along the cochlea, 6-FAM-ZOL-treated bone along the osseous spiral lamina of the modiolus exhibited a steeper gradient of fluorescence from base to apex (difference between regression line slopes $p<0.0001$), while no significant gradient was seen for measurements taken along the lateral wall of the same cochleae (difference between regression line slopes $p=0.09$). However, both the modiolus and the lateral wall had levels of fluorescence that were significantly higher than the control (Figure 5A–B). Critically, we observed no shifts in ABR or DPOAE three weeks after placement of 6-FAM-ZOL on the RWM (Supp Figure 2). We concluded that placement of 30% of the 1X systemic 6-FAM-ZOL dose onto the RWM results in equivalent deposition of 6-FAM-ZOL in the lateral cochlear wall relative to the 1X systemic dose, and that local delivery of 6-FAM-ZOL in this manner was not ototoxic.

Direct intracochlear infusion of zoledrenate (6-FAM-ZOL) was by far the most efficient delivery mode

Finally, we infused 6-FAM-ZOL directly into the cochlea via a cochleostomy using a microfluidic pump. Following delivery of 2% (0.02X) of the 1X systemic 6-FAM-ZOL dose, we identified bright fluorescent signal along both the osseous spiral lamina of the modiolus and the lateral wall of the cochlea (Figure 6). In addition, both the modiolus and the lateral wall exhibited significantly steeper gradients of signal from base to apex compared to the controls (Figure 7; difference between regression line slopes $p<0.0001$). In control animals, we observed a small CAP shift above 12 kHz associated with the cochleostomy and injection procedure, while no significant DPOAE shift was seen (Supp Figure 3). In the 6-FAM-ZOL 0.02X-treated animals we identified a small additional shift in both CAP and DPOAE, in the range of 10–15 dB. We therefore carried out additional cochleostomy delivery experiments infusing native zoledronate mixed with 6-FAM-ZOL to double the delivered bisphosphonate concentration to 0.04X. These animals showed no shift relative to control animals (Supp Fig 3). Direct infusion of 6-FAM-ZOL into the cochlea therefore results in very high levels of delivery relative to systemic or RWM delivery, and such delivery can be achieved without significant immediate ototoxicity.

DISCUSSION

We have employed a novel, fluorescently labelled bisphosphonate compound (6-FAM-ZOL) *in vivo* to demonstrate that bisphosphonates distribute to otic capsule when systemically delivered. We further show that an alginate hydrogel system can deliver 6-FAM-ZOL throughout the cochlea when delivered to the round window. Finally, we achieved the most efficient delivery of 6-FAM-ZOL to cochlear bone upon direct cochlear infusion via a

cochleostomy. Bisphosphonate delivery did not damage the cochlea over the course of our experiments, as assessed by hearing measurements.

Previous animal studies have employed other fluorescently labelled bisphosphonate compounds to evaluate bisphosphonate delivery and assess bisphosphonate retention within appendicular and mandibular bone (28,29). Our work extends these findings to evaluate the amount of bisphosphonate delivered to the otic capsule following systemic administration. We found that the amount of bisphosphonate taken up by the otic capsule was lower than that taken up by the tibia (approximately 2/3 as much). This difference likely reflects the fact that bisphosphonates are taken up by osteoclasts associated with bone resorption cavities involved in bone remodeling (16) and that, unlike the tibia and other bones, normal otic capsule bone does not undergo significant remodeling (30). Further experiments are required to assess whether or not the uptake of bisphosphonate is higher in otic capsule bone that is actively undergoing abnormal turnover, such as occurs in otosclerosis. If so, 6-FAM-ZOL could be useful as a probe to identify areas of active bone turnover in future animal models for otosclerosis. Similar bisphosphonate probes have been used to evaluate the cellular and skeletal distribution of bisphosphonates *in vivo* (31–36).

One goal of this study was to identify a local delivery dose for 6-FAM-ZOL that mirrors the dose delivered to the cochlea upon systemic administration of the equivalent human dose by weight. We found that approximately 30% of the 1X systemic dose delivered to the round window by an alginate hydrogel resulted in similar fluorescence within the lateral cochlear wall relative to the 1X systemic dose, while delivery of only 2% of the 1X systemic dose of 6-FAM-ZOL through a cochleostomy resulted in comparable levels of fluorescence. Interestingly, when 6-FAM-ZOL was delivered directly into the scala tympani, the osseous spiral lamina appeared to take up bisphosphonate more readily than did the lateral wall of the cochlea. We do not yet know if the basis for this difference is of physiologic interest.

Notably, we observed that the fluorescence gradient was significantly steeper from cochlear base to apex along the osseous spiral lamina, but not along the cochlear lateral wall, in cochleae treated with 6-FAM-ZOL via the RWM. However, such a steep gradient was readily observed in both the spiral lamina and lateral wall following 6-FAM-ZOL infusion via a cochleostomy. We hypothesize that diffusion of 6-FAM-ZOL through the mucosa overlying the guinea pig cochlea mitigates the presence of a lateral wall gradient in the setting of RWM delivery. Such diffusion is unlikely to be a relevant mode of entry into the lateral wall of the cochlea in human patients, given the much greater thickness of the otic capsule in the human.

Our results complement analyses of intracochlear concentration gradients that have previously been reported following RWM administration of other compounds, including gentamicin and dexamethasone (37–39). Those studies assessed intracochlear concentrations in “real time” by directly sampling perilymph, while our method exploits the high bone affinity of 6-FAM-ZOL to estimate the cumulative amount of drug delivered. In this regard, previously reported real-time gradients appear to be steeper than the ones we observed, although differences in the mode of drug delivery likely also affect the shape of these curves. Notably, our RWM delivery experiments also showed evidence of drug delivery

through the oval window (data not shown), reflecting the very close proximity of the two windows in the guinea pig. Our present findings therefore provide a fuller understanding of the extent and location of drug delivery to the cochlea.

The system we have established, which relies on direct visualization of bisphosphonate binding via undemineralized processing of otic capsule bone, allows for the direct and generalizable assessment of other systems for cochlear drug delivery. Other potential round window delivery systems that could be evaluated in this fashion include poloxamer (40,41), as well as other aqueous solution-based systems (37,42). In addition, other approaches that directly introduce compounds into perilymph, whether through the round window or through a cochleostomy, may also be studied. Other modes of delivery of substances to the middle ear, including emerging transtympanic methods (43), could be evaluated using our methodology.

From a clinical perspective, our findings hold particular relevance for the treatment of cochlear otosclerosis. We anticipate that these findings will inform future studies that will explore new avenues for bisphosphonate delivery. One method that we are actively investigating in this regard is the use of a drug-eluting stapes prosthesis that could be used to deliver bisphosphonates and other drugs, including steroids, into the inner ear. Further work is needed to identify those patients at greatest risk for progression from stapedial otosclerosis to cochlear otosclerosis.

CONCLUSION

We have used a novel, fluorescently labeled bisphosphonate derivative to characterize bisphosphonate delivery to bone of the lateral cochlear wall following systemic injection and local delivery via the RWM and a cochleostomy. These findings lay the groundwork for both pre-clinical and clinical applications for the treatment of cochlear otosclerosis.

Supplementary Material

Refer to Web version on PubMed Central for supplementary material.

Acknowledgments

We thank Doug Hayden, PhD, for assistance with the biostatistical analyses, and Kris Kristiansen for excellent technical support. This work was primarily supported by NIDCD grant R01 DC009837, with additional support from Harvard Catalyst | The Harvard Clinical and Translational Science Center (National Center for Research Resources and the National Center for Advancing Translational Sciences, National Institutes of Health Award 8UL1TR000170-05, and financial contributions from Harvard University and its affiliated academic health care centers).

References

1. Chole RA, McKenna M. Pathophysiology of otosclerosis. Otol Neurotol. 2001; 22:249–57. [PubMed: 11300278]
2. Doherty JK, Linthicum FH. Spiral ligament and stria vascularis changes in cochlear otosclerosis: effect on hearing level. Otol Neurotol. 2004; 25:457–64. [PubMed: 15241221]
3. Ealy M, Smith RJ. Otosclerosis. Adv Otorhinolaryngol. 2011; 70:122–9. [PubMed: 21358194]

4. Quesnel AM, Seton M, Merchant SN, et al. Third-generation bisphosphonates for treatment of sensorineural hearing loss in otosclerosis. Otol Neurotol. 2012; 33:1308–14. [PubMed: 22935809]
5. Balle V, Linthicum FH. Histologically proven cochlear otosclerosis with pure sensorineural hearing loss. Ann Otol Rhinol Laryngol. 1984; 93:105–11. [PubMed: 6712083]
6. Semaan MT, Gehani NC, Tummala N, et al. Cochlear implantation outcomes in patients with far advanced otosclerosis. Am J Otolaryngol. 2012; 33:608–14. [PubMed: 22762960]
7. Ramsden R, Rotteveel L, Proops D, et al. Cochlear implantation in otosclerotic deafness. Adv Otorhinolaryngol. 2007; 65:328–34. [PubMed: 17245067]
8. Marshall AH, Fanning N, Symons S, et al. Cochlear implantation in cochlear otosclerosis. Laryngoscope. 2005; 115:1728–33. [PubMed: 16222185]
9. Rama-Lopez J, Cervera-Paz FJ, Manrique M. Cochlear implantation of patients with far-advanced otosclerosis. Otol Neurotol. 2006; 27:153–8. [PubMed: 16436983]
10. Clayton AE, Mikulec AA, Mikulec KH, et al. Association between osteoporosis and otosclerosis in women. J Laryngol Otol. 2004; 118:617–21. [PubMed: 15453937]
11. McKenna MJ, Nguyen-Huynh AT, Kristiansen AG. Association of otosclerosis with Sp1 binding site polymorphism in COL1A1 gene: evidence for a shared genetic etiology with osteoporosis. Otol Neurotol. 2004; 25:447–50. [PubMed: 15241219]
12. Santos F, McCall AA, Chien W, et al. Otopathology in Osteogenesis Imperfecta. Otol Neurotol. 2012; 33:1562–6. [PubMed: 22996160]
13. Khetarpal U, Schuknecht HF. In search of pathologic correlates for hearing loss and vertigo in Paget's disease. A clinical and histopathologic study of 26 temporal bones. Ann Otol Rhinol Laryngol Suppl. 1990; 145:1–16. [PubMed: 2106820]
14. Lipton A. New therapeutic agents for the treatment of bone diseases. Expert Opin Biol Ther. 2005; 5:817–32. [PubMed: 15952912]
15. Bellido T, Plotkin LI. Novel actions of bisphosphonates in bone: preservation of osteoblast and osteocyte viability. Bone. 2011; 49:50–5. [PubMed: 20727997]
16. Allen MR, Burr DB. Bisphosphonate effects on bone turnover, microdamage, and mechanical properties: what we think we know and what we know that we don't know. Bone. 2011; 49:56–65. [PubMed: 20955825]
17. accessdata.fda.gov. Full Prescribing Information for Reclast (zoledronic acid). 2011
18. Papapetrou PD. Bisphosphonate-associated adverse events. Hormones (Athens). 2009; 8:96–110. [PubMed: 19570737]
19. Silverman SL, Landesberg R. Osteonecrosis of the jaw and the role of bisphosphonates: a critical review. Am J Med. 2009; 122:S33–45. [PubMed: 19187811]
20. Lewiecki EM. Safety of long-term bisphosphonate therapy for the management of osteoporosis. Drugs. 2011; 71:791–814. [PubMed: 21504254]
21. Whitaker M, Guo J, Kehoe T, et al. Bisphosphonates for osteoporosis--where do we go from here? N Engl J Med. 2012; 366:2048–51. [PubMed: 22571168]
22. Russell RG. Bisphosphonates: mode of action and pharmacology. Pediatrics. 2007; 119 (Suppl 2):S150–62. [PubMed: 17332236]
23. Kashemirov BA, Bala JL, Chen X, et al. Fluorescently labeled risedronate and related analogues: "magic linker" synthesis. Bioconjug Chem. 2008; 19:2308–10. [PubMed: 19032080]
24. Sun S, Błazewska KM, Kashemirov BA, et al. Synthesis and characterization of novel fluorescent nitrogen-containing bisphosphonate imaging probes for bone active drugs. Phosphorus Sulfur Silicon Relat Elem. 2011; 186:970–1. [PubMed: 21894242]
25. Sun, S. Chemistry. Los Angeles: University of Southern California; 2013. Fluorescent imaging probes of nitrogen-containing bone active drugs: design, synthesis, and applications.
26. Chen T, Berenson J, Vescio R, et al. Pharmacokinetics and pharmacodynamics of zoledronic acid in cancer patients with bone metastases. J Clin Pharmacol. 2002; 42:1228–36. [PubMed: 12412821]
27. Rasband, WS. ImageJ. U. S. National Institutes of Health; Bethesda, Maryland, USA: 1997–2014. http://imagej.nih.gov/ij/

28. Kozloff KM, Volakis LI, Marini JC, et al. Near-infrared fluorescent probe traces bisphosphonate delivery and retention in vivo. J Bone Miner Res. 2010; 25:1748–58. [PubMed: 20200982]
29. Wen D, Qing L, Harrison G, et al. Anatomic site variability in rat skeletal uptake and desorption of fluorescently labeled bisphosphonate. Oral Dis. 2011; 17:427–32. [PubMed: 21122034]
30. Frisch T, Sorensen MS, Overgaard S, et al. Estimation of volume referent bone turnover in the otic capsule after sequential point labeling. Ann Otol Rhinol Laryngol. 2000; 109:33–9. [PubMed: 10651409]
31. Roelofs AJ, Stewart CA, Sun S, et al. Influence of bone affinity on the skeletal distribution of fluorescently labeled bisphosphonates in vivo. J Bone Miner Res. 2012; 27:835–47. [PubMed: 22228189]
32. Roelofs AJ, Coxon FP, Ebetino FH, et al. Fluorescent risedronate analogues reveal bisphosphonate uptake by bone marrow monocytes and localization around osteocytes in vivo. J Bone Miner Res. 2010; 25:606–16. [PubMed: 20422624]
33. Hokugo A, Sun S, Park S, et al. Equilibrium-dependent bisphosphonate interaction with crystalline bone mineral explains anti-resorptive pharmacokinetics and prevalence of osteonecrosis of the jaw in rats. Bone. 2013; 53:59–68. [PubMed: 23219943]
34. Vermeer JA, Jansen ID, Marthi M, et al. Jaw bone marrow-derived osteoclast precursors internalize more bisphosphonate than long-bone marrow precursors. Bone. 2013; 57:242–51. [PubMed: 23962725]
35. Bae S, Sun S, Aghaloo T, et al. Development of oral osteomucosal tissue constructs in vitro and localization of fluorescently-labeled bisphosphonates to hard and soft tissue. Int J Mol Med. 2014; 34:559–63. [PubMed: 24920042]
36. Turek J, Ebetino FH, Lundy MW, et al. Bisphosphonate binding affinity affects drug distribution in both intracortical and trabecular bone of rabbits. Calcif Tissue Int. 2012; 90:202–10. [PubMed: 22249525]
37. Plontke SK, Biegner T, Kammerer B, et al. Dexamethasone concentration gradients along scala tympani after application to the round window membrane. Otol Neurotol. 2008; 29:401–6. [PubMed: 18277312]
38. Mynatt R, Hale SA, Gill RM, et al. Demonstration of a longitudinal concentration gradient along scala tympani by sequential sampling of perilymph from the cochlear apex. J Assoc Res Otolaryngol. 2006; 7:182–93. [PubMed: 16718612]
39. Plontke SK, Mynatt R, Gill RM, et al. Concentration gradient along the scala tympani after local application of gentamicin to the round window membrane. Laryngoscope. 2007; 117:1191–8. [PubMed: 17603318]
40. Wang X, Dellamary L, Fernandez R, et al. Principles of inner ear sustained release following intratympanic administration. Laryngoscope. 2011; 121:385–91. [PubMed: 21271594]
41. Wang X, Fernandez R, Tsivkovskaia N, et al. OTO-201: Nonclinical Assessment of a Sustained-Release Ciprofloxacin Hydrogel for the Treatment of Otitis Media. Otol Neurotol. 2014; 35:459–69. [PubMed: 24518407]
42. Lajud SA, Han Z, Chi FL, et al. A regulated delivery system for inner ear drug application. J Control Release. 2013; 166:268–76. [PubMed: 23313113]
43. Khoo X, Simons EJ, Chiang HH, et al. Formulations for trans-tympanic antibiotic delivery. Biomaterials. 2013; 34:1281–8. [PubMed: 23146430]

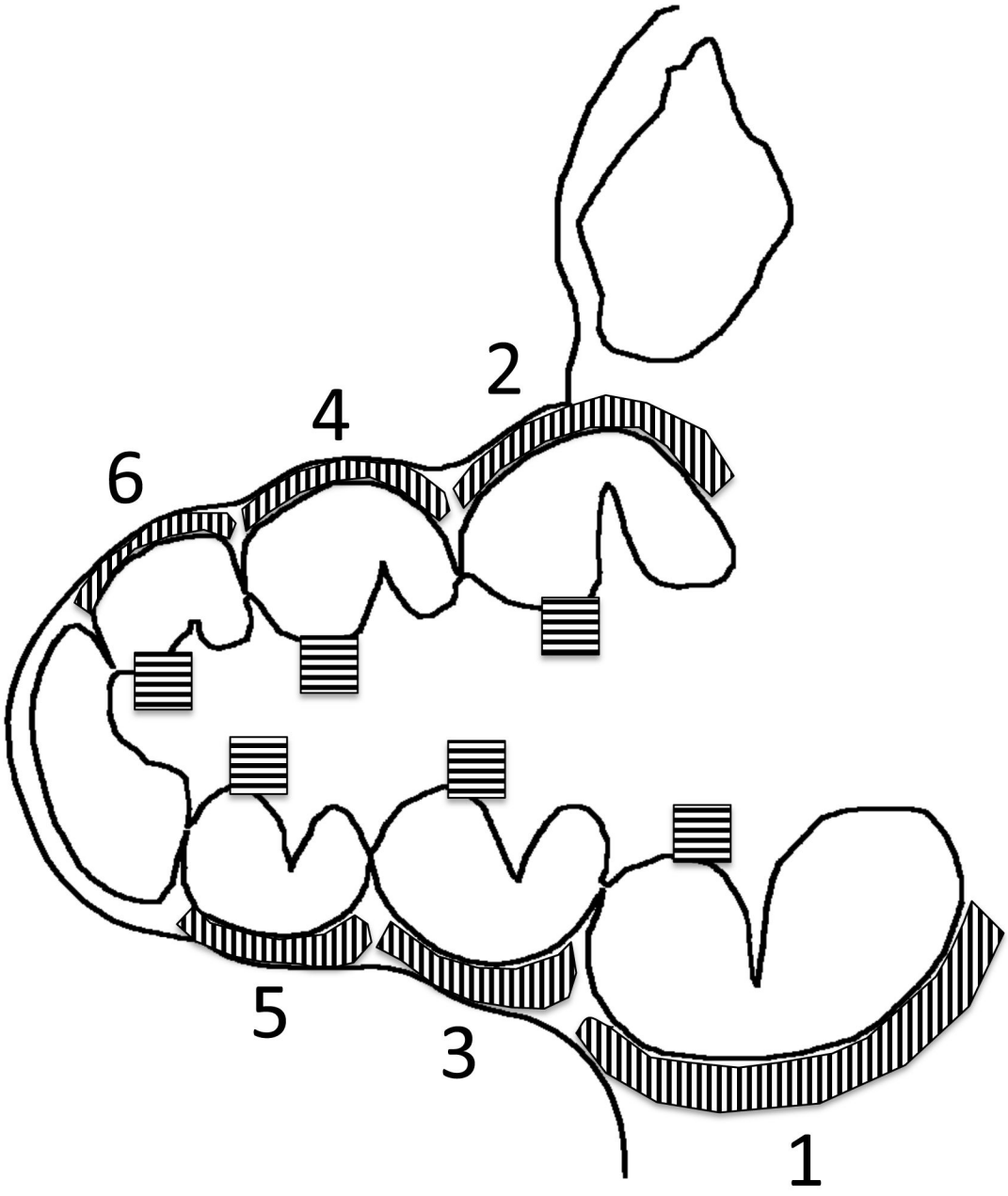

Fig. 1. Measurement of lateral cochlear wall fluorescence

Depicted is a schematic of the guinea pig cochlea taken at a mid-modiolar section. Shaded areas of the modiolus and lateral cochlear wall at each half-turn were measured for average fluorescence. Average fluorescence measurements were taken along each cochlear half-turn at the mid-modiolar section (schematic in Figure 1).

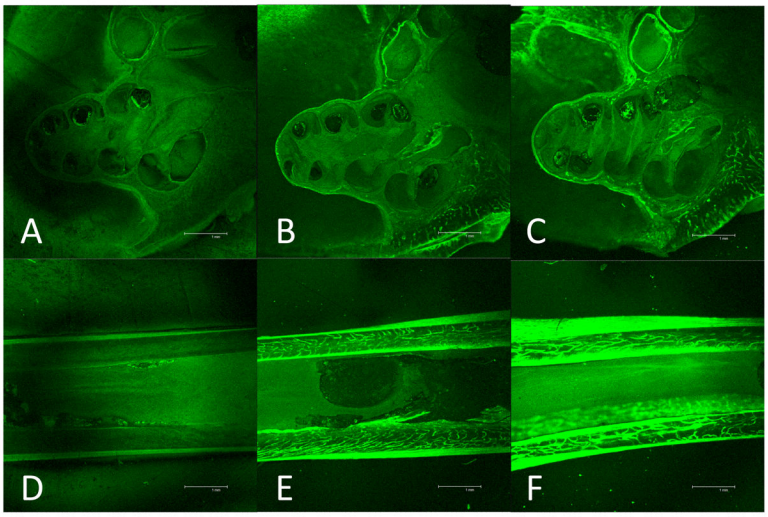

Fig. 2. Systemic delivery of 6-FAM-ZOL

Fluorescent photomicrographs taken at mid-modiolar cochlear sections are shown for untreated cochlea (A), treatment with 1X the human zoledronate dose by molar mass (B), and treatment with 3X the human zoledronate dose by molar mass (C). Fluorescent photomicrographs of tibial sections are shown for untreated tibia (D), treatment with 1X the human dose (E), and treatment with 3X the human dose (F).

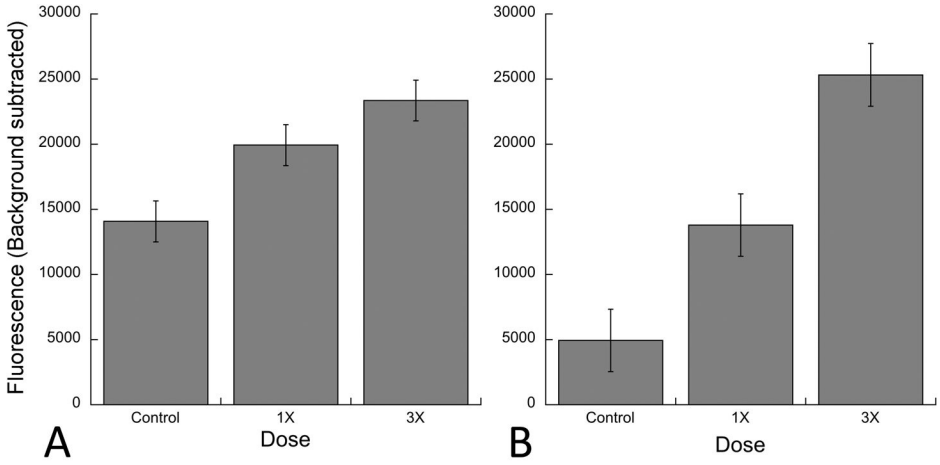

Fig. 3. Quantification of fluorescence following systemic 6-FAM-ZOL treatment

Measurements are shown for cochleae (A) and tibeae (B). For cochleae, measurements were taken at each of six cochlear half-turns from base to apex and averaged. The data summarize three independent experiments for tibiae and seven independent experiments for cochleae. Statistical significance was measured using ANOVA. For the lateral wall, the p values between control and 1X, control and 3X, and 1X and 3X were 0.016, <0.0001, and 0.0352 respectively.

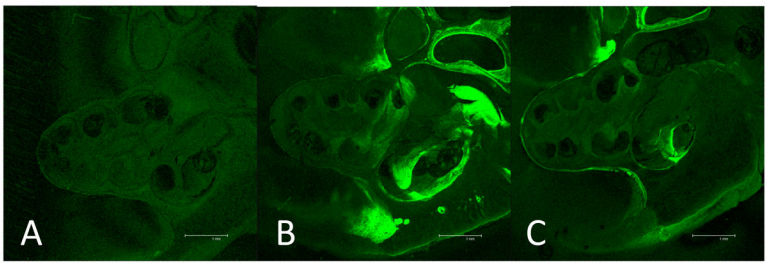

Fig. 4. RWM delivery of 6-FAM-ZOL

Fluorescent photomicrographs taken at mid-modiolar sections of the cochlea are shown for untreated cochlea (A), treatment with 10% of the 1X systemic dose (B), and treatment with 30% of the 1X systemic dose (C). The increased signal outside the RW niche in B was seen in some trials but was not consistently reproducible and represents minor spillover from the niche.

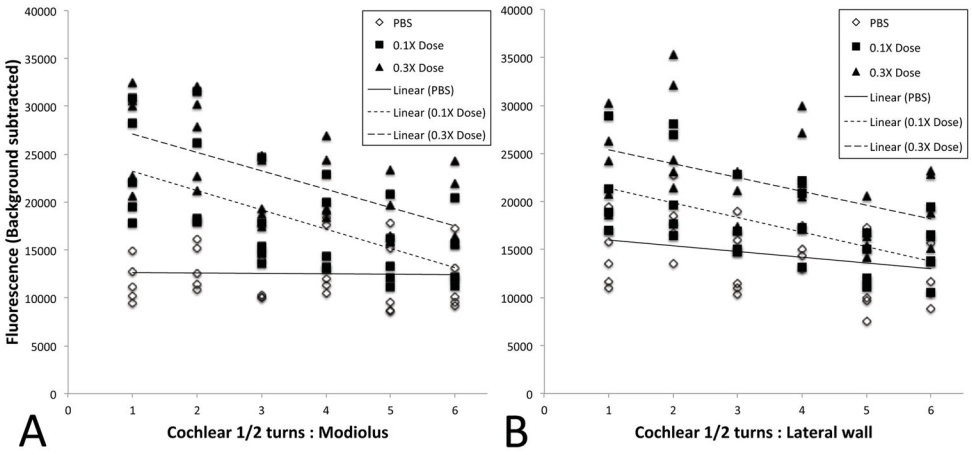

Fig. 5. Quantification of fluorescence following RWM 6-FAM-ZOL treatment

Measurements were taken at each of six cochlear half-turns from base to apex, along both the modiolus (A) and lateral wall (B). Data points from all experiments are shown, along with the best-fit regression plot. For the lateral wall, the p values for total average fluorescence between control and 0.1X, control and 0.3X, and 0.1X and 0.3X were 0.018, 0.0001, and 0.0038 respectively, while for the modiolus, the p values for total average fluorescence between control and 1X, control and 3X, and 1X and 3X were 0.0040, 0.0001, and 0.0194 respectively. Slopes of the 0.1X and 0.3X regression lines were significantly different from the slope of the control along the modiolus ($p<0.0001$), while for the lateral wall the slopes were not significantly different ($p=0.09$).

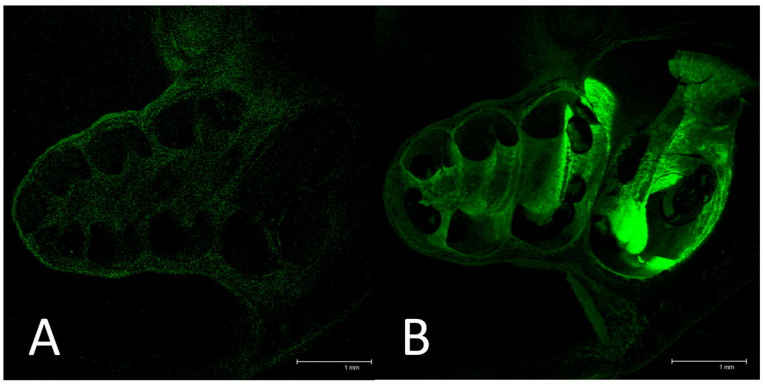

Fig. 6. Direct cochlear infusion of 6-FAM-ZOL

Fluorescent photomicrographs taken at mid-modiolar sections of the cochlea are shown for untreated cochlea (A) and treatment with 2% of the 1X systemic dose (B).

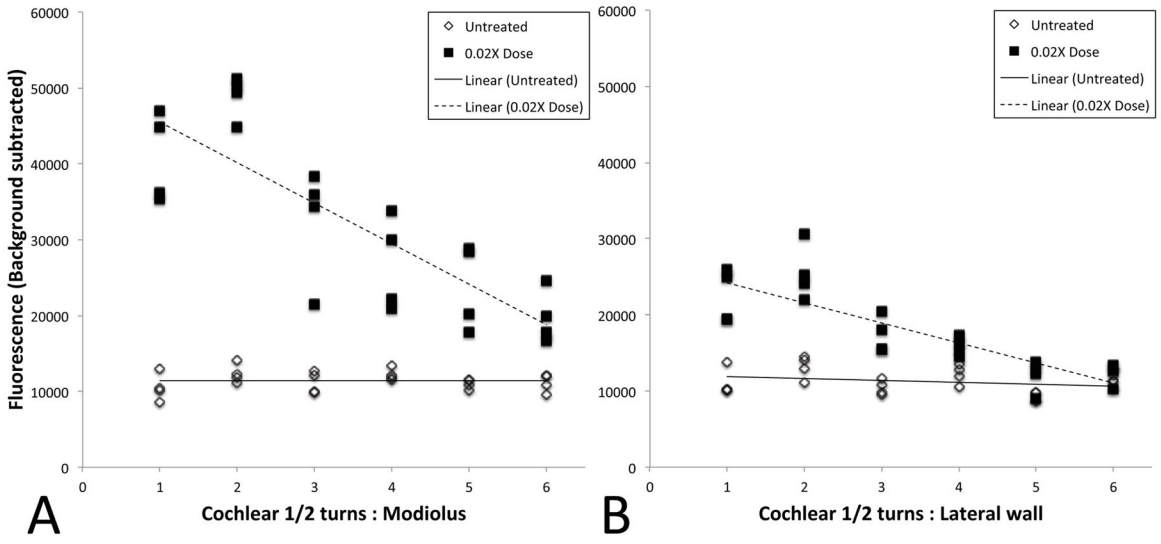

Fig. 7. Quantification of fluorescence following cochlear infusion of 6-FAM-ZOL

Measurements were taken at each of six cochlear half-turns from base to apex, along both the modiolus (A) and lateral wall (B). Data points from all experiments are shown, along with the best-fit regression plot. Total average fluorescence was significantly greater in 0.02X for both the modiolus ($p=0.0031$), the lateral wall ($p=0.0124$). The slope of the 0.02X regression plot was significantly different from the control for both the modiolus ($p=0.0003$) and the lateral wall ($p=0.0007$).